Multispectral and lifetime imaging for the detection of skin tumors

Cubeddu, R; Pifferi, A; Taroni, P; Valentini, G; Canti, G; Lindquist, C; Andersson-Engels, Stefan; Svanberg, Sune; Wang, I; Svanberg, Katarina

Published in:
Biomedical Optical Spectroscopy and Diagnostics / Therapeutic Laser Applications. Proc. OSA Trends in Optics and Photonics

1998

Multispectral and lifetime imaging for the detection of skin tumors

Rinaldo Cubeddu, Antonio Pifferi, Paola Taroni, and Gianluca Valentini
CEQSE-CNR and INFM-Dipartimento di Fisica, Politecnico di Milano, Piazza Leonardo da Vinci 32, 20133 Milano, Italy

Gianfranco Canti
Department of Pharmacology, Università di Milano, Via Vanvitelli 32, I-20129 Milano, Italy

Charlotta Lindquist, Stefan Andersson-Engels, and Sune Svanberg
Department of Physics, Lund Institute of Technology, P.O. Box 118, S-221 00 Lund, Sweden

Ingrid Wang, and Katarina Svanberg
Department of Oncology, Lund University Hospital, S-221 85 Lund, Sweden

Abstract

Multispectral and lifetime imaging systems have been used to detect skin cancer in humans after the topical application of δ-aminolevulinic acid ointment. Both systems allowed a clear detection of tumors based either on spectral or on temporal differences between the fluorescence signals in the neoplasia and in the healthy tissues nearby.

Key Words

(170.0110) Imaging systems; (300.2530) Fluorescence, laser-induced; (170.3650) Lifetime-based sensing; (170.1870) Dermatology.

Introduction

Since several years ago, fluorescence spectroscopy and imaging were being used for the detection of cancer based on endogenous or exogenous fluorophores. Researchers, who often have to deal with weak and relatively unspecific fluorescence emission, have always been looking for an effective selectivity criterion to discriminate neoplastic from healthy tissue. Working with exogenous fluorescent dyes, selectivity criteria have been successfully found both in the spectral and in the time domains. In the first case, two or more images are acquired with different spectral filters and a suitable algorithm, based on image subtraction and/or ratioing, leads to a pseudoimage where areas with pixel values exceeding a predefined threshold value are marked as neoplastic ones [1,2]. This approach takes advantage of the reduction in natural fluorescence accompanied by the increase in fluorescence of exogenous markers that has been frequently observed in neoplastic tissues.

Whenever exogenous fluorophores are characterized by lifetimes different from the ones typical of the natural tissue fluorescence and when they accumulate more in pathologic areas, cancer detection can be performed, at least in principle, in the time domain as well. As an example, this is the case of some exogenous photosensitizers for the photodynamic therapy of tumors, such as Porphyrins, whose fluorescence lifetime is of about 10-15 ns, typically longer than observed in untreated tissues.

If the exogenous fluorophores are accumulated in tumors with high selectivity, a simple time gated acquisition can lead to a successful detection of pathologic areas. In some conditions, when time gating is not effective due to the limited selectivity, a difference in the exogenous fluorescence lifetimes can be exploited to discriminate the neoplastic tissue from the healthy one [3]. This can be the case for porphyrin-based compounds, which are made of a mixture of monomers, dimers and oligomers. The biochemical differences between the tumor and the healthy tissue account for a significant increase in the fluorescence lifetime in the tumor even though the fluorescence intensity is unspecific. The tumor detection can thus be carried out by a system capable to calculate the spatial distribution of the fluorescence decay time, that is a lifetime image.

The present work has been devised to evaluate the diagnostic capabilities of two imaging systems working in the spectral and in the time domains, respectively. The sensitizer used was δ-aminolevulinic acid (ALA), a precursor of the naturally occurring fluorescent agent Protoporphyrin IX, and the investigation was carried out at the Lund University Medical Laser Centre on patients affected by skin cancer.

Materials and Methods

Two patients affected by previously assessed Basal Cell Carcinomas (BCCs) (total of 5 lesions) were treated with

OSA TOPS Vol 22 Biomedical Optical Spectroscopy and Diagnostics / Therapeutic Laser Applications, Eva M. Sevick-Muraca, Joseph A. Izatt, and Marwood N. Ediger (eds.)

topical application of 20% ALA ointment 2 hours before the fluorescence measurements.

A preliminary fluorescence investigation was carried out using a Nitrogen pumped dye laser and an optical multichannel analyzer (OMA). An optical fiber in contact with the skin was used to deliver the excitation light and to collect the fluorescence signal. Two point measurements were performed on each BCC: the first one in the center of the lesion, the second a few millimeters outside.

Thereafter, a multicolor and a lifetime image of each lesion were acquired in sequence, using the experimental setups described in the following.

Multicolor Imaging System

Multicolor imaging was carried out by taking three spatially identical, but spectrally different images with the same intensified CCD camera, using a system developed for endoscopic applications. The images were spectrally separated by means of dichroic mirrors in three wavelength bands. One (named A) was in the red area, one (B) in the blue area, and one (D) in the green-yellow area. The fluorescence was induced by means of ultraviolet light (390 nm) from a frequency-doubled Alexandrite laser. The laser light was delivered by an optical fiber and the fluorescence was detected through an endoscope. The gated image intensifier was synchronized with the laser. Thereby, the normal reflected light image could also be recorded simultaneously by a color CCD camera on the endoscope adapter. The fluorescence image was digitized and kept in a frame grabber in a PC/486 computer. Calculations were subsequently carried out on the digitized image. The function

with A, B, and D defined above and k_1 and k_2 being constants with different values for different applications, was used to produce a pseudocolor image with a high contrast between normal and malignant tumor tissue. The PC computed the F_c value pixel by pixel and fed the result via an output frame grabber to a video mixer, where the pseudocolor fluorescence image could be mixed with the normal image from the color CCD camera.

Lifetime Imaging System

The lifetime imaging system is essentially made of a Nitrogen pumped dye laser, emitting 1 ns pulses at 405 nm, and an intensified CCD video camera, whose light amplifier can be gated with a gate rise time of 2 ns. A precision delay generator and some electronic devices complete the system. The images were acquired and processed by high performance image boards in a personal computer.

In the present experiment, four images per sample were acquired, after the delays of 0, 5, 10, and 20 ns (with respect to the excitation pulses). Then the images were processed according to the algorithm described in the following.

Based on a simplified model, the measured fluorescence signal I(t) can be assumed to be roughly monoexponential. Image acquisition corresponds to time integration and spatial sampling, which lead to the following matrix representation of the irradiance $H_{i,j}$:

$$H_{i,j}(d_k) = k\int_{t_d}^{\infty} I_{i,j}(t)dt = C\tau_{i,j}I_{i,j}(0)\exp\left(-d_k/\tau_{i,j}\right),$$

where subscripts i,j refer to image pixels, d_k is the delay (0, 5, 10 or 20 ns), $\tau_{i,j}$ is the decay time matrix, $I_{i,j}(0)$ is the matrix of the corresponding fluorescence intensity immediately after the excitation pulse, and C is a system dependent constant. The spatial distribution of the decay time $\tau_{i,j}$ can be calculated by doing a simple linear regression:

$$\frac{1}{\tau_{i,j}} = -\frac{n\cdot\sum_k d_k\cdot\ln H_{i,j}(d_k) - \sum_k d_k\cdot\sum_k \ln H_{i,j}(d_k)}{n\cdot\sum_k d_k^2 - \left(\sum_k d_k\right)^2},$$

where n is the number of delays.

Then, the amplitude matrix is given by:

$$A_{i,j} = \frac{H_{i,j}(d_0)}{\tau_{i,j}\cdot\exp(-d_0/\tau_{i,j})}.$$

Finally, $\tau_{i,j}$ and $A_{i,j}$ can be plotted in gray shade or pseudocolor images.

Results and Discussion

Figure 1 shows two typical OMA spectra taken in the center of the lesion (Figure 1a) and 4 mm outside (Figure 1b). In both cases, the short wavelength rise is caused by the cut-off filter, which is used to remove the scattered laser light. The blue-green signal is due to the natural tissue fluorescence and is significantly lower in the spectrum acquired from the lesion than 4 mm outside it. In the center of the lesion the dominant peak, which corresponds to the induced Protoporphyrin IX emission, is centered at 635 nm. No contribution to the spectrum comes from porphyrins in the case of healthy tissues. The reduction in natural fluorescence and the presence of the exogenous signal are typical findings in cancerous tissues, which can be profitably used for tumor detection in the spectral domain.

Figure 2 shows a white light image of the same lesion as considered above, taken with the fluorescence camera (Figure 2a) and the corresponding multicolor image (Figure 2b). In the white light image, two areas can be identified as darker than the background: the one on the left is a benign nevus, while the one on the right is the

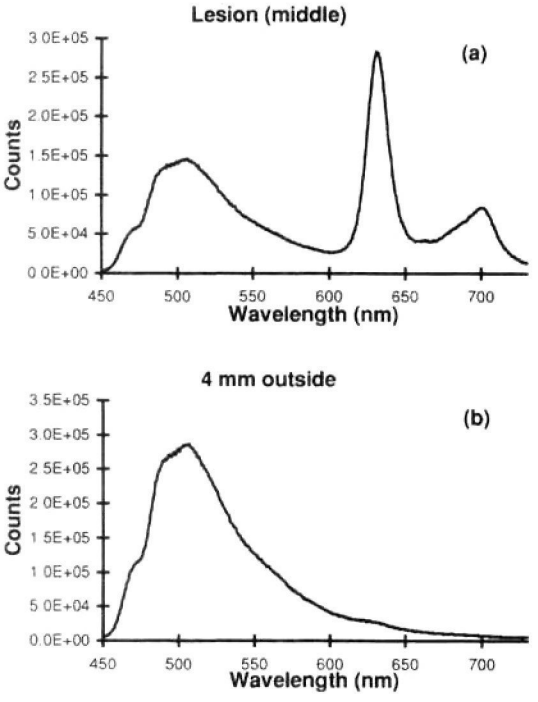

Figure 1. Fluorescence spectra acquired under 390 nm excitation from the center of a BCC (a) and 4 mm outside (b).

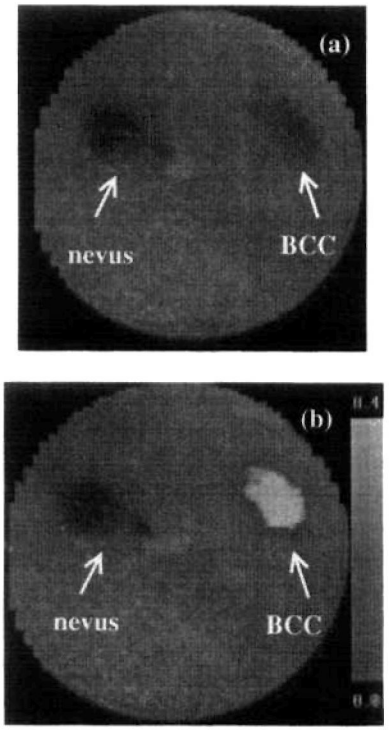

Figure 2. White light (a) and multicolor (b) images of a BCC (see Figure 1) and a benign nevus.

BCC, as it could be easily assessed by a visual examination of the patient. In the multicolor image, the BCC emerges from the background with sharply defined margins, while the nevus still remains darker than the healthy skin, allowing the detection of the malignant lesion and its discrimination from the benign one.

Figure 3 shows images of the same lesion as considered before, taken by means of the time resolved imaging system. Figures 2 and 3 show a left-right inversion and an unlike magnification since they have been recorded through completely different optical devices (endoscope and macro lens, respectively). Figure 3a is a map of the fluorescence lifetimes calculated using the four delayed images, while Figure 3b shows the spatial distribution of the corresponding amplitudes. It is well known that the Protoporphyrin IX emission is characterized by a long lifetime ($\tau > 15$ ns), while the other components of tissue fluorescence are short living ($\tau \leq 5$ ns). The bright spot in Figure 3a corresponds to the lesion and the light gray area surrounding it coincides with the region over which the ALA was applied. On the other hand, the healthy skin (including the nevus) is dark. As evident from Figure 3a, the estimated lifetimes are in the range of 8 to 18 ns. All these pieces of information indicate that the porphyrin emission dominates the image.

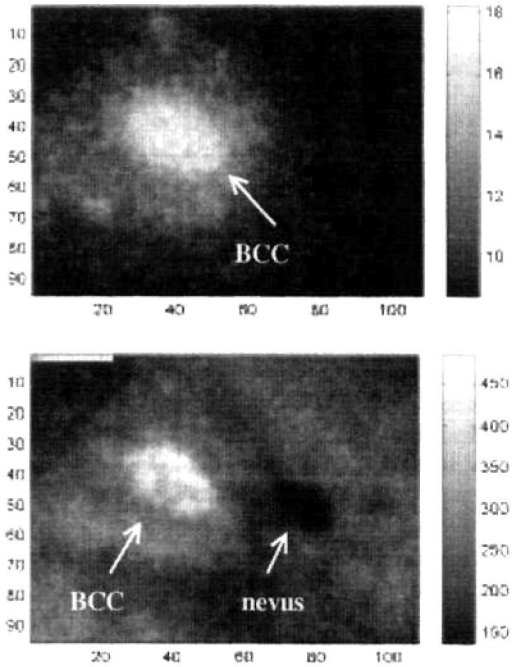

Figure 3. Fluorescence lifetime (a) and amplitude (b) images of the same BBC as shown in Figure 2.

The Protoporphyrin IX is induced over all the area covered by the cream, but significantly longer lifetimes are detected in the lesion. This is in agreement with previous results. Actually, in a systematic study performed with

experimental tumors in mice sensitized with Hematoporphyrin Derivative, it has been observed that a significant lengthening of the porphyrin fluorescent lifetime takes place in the tumor [4]. The distribution of fluorescence amplitudes reported in Figure 3b again allows a clear localization of the tumor area. In this case, the detection of the lesion is based on the fact that porphyrins are induced at a higher concentration in the neoplastic tissue than in the surrounding healthy skin, leading to a bright spot, which demarcates the pathologic tissue.

In conclusion, based on these preliminary findings, both the multicolor and the lifetime imaging systems allow a reliable detection of basaliomas in patients sensitized with ALA. Further studies are in progress to confirm the results obtained so far and investigate more in detail the diagnostic potential of the two techniques.

References

1. S. Andersson-Engels, J. Johansson and S. Svanberg, "Medical diagnostic system based on simultaneous multispectral fluorescence imaging", Appl. Opt. 34 8022-8026 (1994).
2. K. Svanberg, I. Wang, S. Colleen, et al., "Clinical Multi-Colour Fluorescence Imaging of Malignant Tumours -Initial Experience," Acta Radiol. 38 (1997), in press.
3. R.Cubeddu, A.Pifferi, P.Taroni, G.Valentini and G.Canti, "Tumor detection in mice by measurements of fluorescence decay time matrices," Opt. Lett. 20 2553-2555 (1995).
4. R.Cubeddu, G.Canti, A.Pifferi, P.Taroni and G.Valentini, "Fluorescence lifetime imaging of experimental tumours in HpD-sensitised mice," Photochem. Photobiol. 66 229-236 (1997).